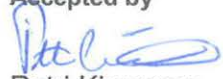


## Effect of hydrazine on carbon steel corrosion under PWR secondary side conditions

Authors: Konsta Sipilä, Saija Väisänen and Timo Saario

Confidentiality: Public

<b>Report's title</b>	
Effect of hydrazine on carbon steel corrosion under PWR secondary side conditions	
<b>Customer, contact person, address</b>	<b>Order reference</b>
SAFIR 2014 Research Programme / Fortum Power and Heat Oy	3182LO13
<b>Project name</b>	<b>Project number/Short name</b>
Water chemistry and plant availability	77488 / WAPA
<b>Author(s)</b>	<b>Pages</b>
Konsta Sipilä, Saija Väisänen and Timo Saario	15/
<b>Keywords</b>	<b>Report identification code</b>
Carbon steel, hydrazine, corrosion	VTT-R-00510-14
<b>Summary</b>	
<p>The effect of hydrazine on corrosion rate of low-alloyed steel (LAS) was studied by in situ and ex situ techniques under PWR secondary side water chemistry conditions at <math>T = 228^{\circ}\text{C}</math> and <math>\text{pH}_{\text{RT}} = 9.2</math> (adjusted by <math>\text{NH}_3</math>). Based on the results the following conclusions can be made:</p> <ul style="list-style-type: none"> <li>Hydrazine injection to a maximum level of 150 ppb onto previously oxidised surface does not affect the corrosion rate of LAS</li> <li>Hydrazine at the level of 100 ppb decreases markedly the amount and the size of deposited oxide crystals on LAS surface. This supports the hypothesis that hydrazine increases magnetite solubility.</li> <li>An oxide grown in the presence of 100 ppb hydrazine shows somewhat weaker protective properties resulting in a higher corrosion rate compared to an oxide film grown without hydrazine. This could explain the accelerating effect of higher concentrations of hydrazine found in flow assisted corrosion (FAC) studies of LAS.</li> </ul>	
<b>Confidentiality</b>	Public
Espoo 31.1.2014	
<b>Written by</b>	<b>Reviewed by</b>
	
Timo Saario Principal Scientist	Ari Koskinen Research Team Leader
	<b>Accepted by</b>
	
	Petri Kinnunen Deputy Research Area Manager
<b>VTT's contact address</b>	
P.O.Box 1000, FI-02044 VTT, Finland	
<b>Distribution (customer and VTT)</b>	
Customer 1 copy, VTT 1 copy	
<p><i>The use of the name of the VTT Technical Research Centre of Finland (VTT) in advertising or publication in part of this report is only permissible with written authorisation from the VTT Technical Research Centre of Finland.</i></p>	

## Preface

---

This research work was performed under the national SAFIR 2014 –research programme as part of the project “Water chemistry and plant availability”. Financial support by Fortum Power and Heat Oy is gratefully acknowledged.

Espoo 31.1.2014

Authors

## Contents

---

Preface.....	2
Contents.....	3
1. Introduction.....	4
2. Goal.....	5
3. Methods.....	5
4. Results.....	7
4.1 Oxide films and weight gain.....	7
4.2 Impedance spectroscopy.....	11
4.3 Polarisation resistance measurements during N <sub>2</sub> H <sub>4</sub> transients.....	12
5. Validation of results.....	15
6. Summary and Conclusions.....	15
References.....	15

## 1. Introduction

Magnetite ( $\text{Fe}_3\text{O}_4$ ) is formed in the secondary circuit of pressurised water reactors (PWR) mainly from corrosion of carbon steel tubing and other carbon steel components. Magnetite particles are transported with the flow and may deposit e.g. in the steam generator (SG) tube support plate and re-heater cassette area possibly creating flow and corrosion problems. Current corrosion problems caused by magnetite deposition include fatigue cracking of SG upper level tubes especially in some plants in France, denting and stress corrosion cracking of SG lower level tubing both in some PWRs and localised corrosion of SG lower level tubing in VVER plants. The remedial measures aim on one hand at reducing the source term, i.e. minimizing carbon steel corrosion and on the other hand at developing water chemistry programs enabling keeping magnetite particles in colloidal form so that they can be more effectively removed via SG blow down.

The corrosion rate of carbon steel depends strongly on  $\text{pH}_{\text{RT}}$  and is at its minimum at  $\text{pH}_{\text{RT}} = 9.8 \dots 10$ . If some components in the secondary side contain copper based materials, the maximum  $\text{pH}_{\text{RT}}$  that can be used is about  $\text{pH}_{\text{RT}} = 9.2$ , because at higher levels of  $\text{pH}_{\text{RT}}$  copper dissolution is drastically accelerated. The  $\text{pH}_{\text{RT}}$  of the secondary side water can be adjusted to the desired level with alkalizing agents, e.g. with ammonia ( $\text{NH}_3$ ) and/or so-called advanced amines (ethanolamine, morpholine etc).

Hydrazine ( $\text{N}_2\text{H}_4$ ) is typically used in PWR secondary side water as an oxygen scavenger. At temperatures higher than about  $T = 150^\circ\text{C}$  hydrazine decomposes producing ammonia. Thus, one option for secondary side water chemistry is  $\text{N}_2\text{H}_4/\text{NH}_3$ . The current view is that hydrazine in larger concentrations can accelerate carbon steel corrosion under flow accelerated corrosion (FAC) conditions. According to EPRI and EdF models /1/, FAC rate in the feed water line would as a maximum roughly double at hydrazine concentration of about 150 to 200 ppb, Figure 1 and Table 1. There have been controversial results in FAC experiments, e.g. Mitsubishi Heavy Industries (MHI) have reported that under similar conditions hydrazine has no effect on FAC /2/.

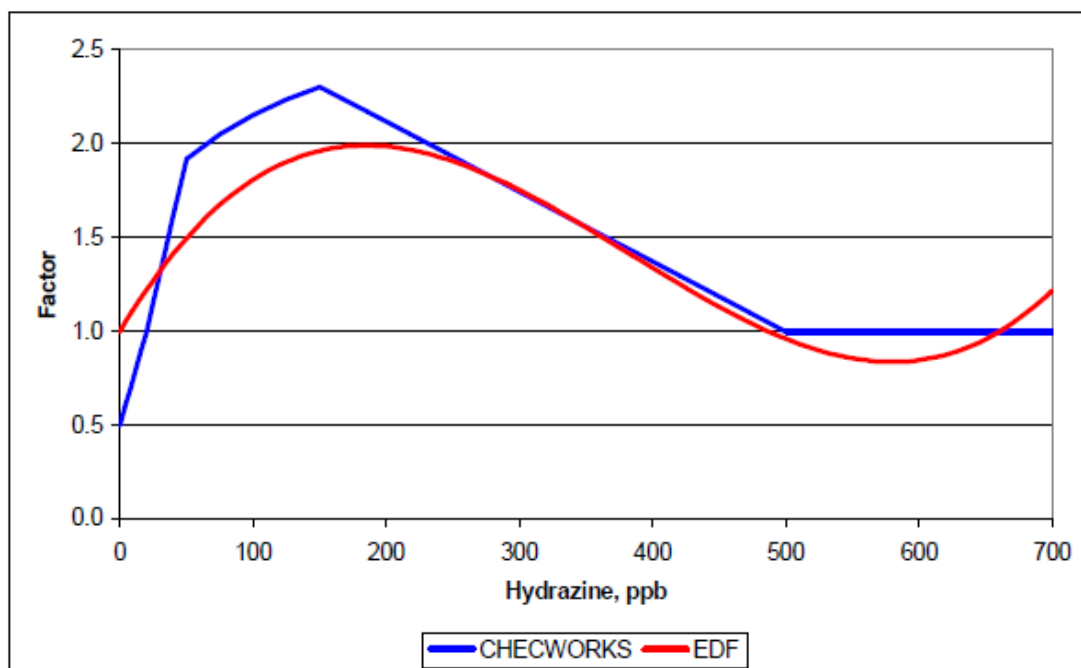


Figure 1 EPRI (Checworks) and EdF models for the effect of hydrazine on carbon steel corrosion under flow accelerated corrosion (FAC) conditions /1 /.

Table 1 Effect of hydrazine concentration and temperature on FAC rate /1/.

Temperature / °C	[N <sub>2</sub> H <sub>4</sub> ] / ppb	Relative FAC rate
180°C	20	1.0
	64	1.5
	280	2.3
225°C	20	1.0
	72	1.9
	390	2.5

In Loviisa nuclear power plant (PWR type VVER 440), the currently used secondary side water chemistry consists of injecting hydrazine at room temperature until a level of 20 ppb is reached at the measurement point near SG entrance. When reaching the limit the injection is stopped and continued when the level has dropped to 2 ppb. Thus, hydrazine level oscillates between 2 and 20 ppb with a frequency of about one hour. According to the EPRI and EdF models, no acceleration of FAC is expected for a maximum 20 ppb concentration of hydrazine.

## 2. Goal

The goal of this study was to clarify effects of hydrazine addition, especially cyclic addition on low-alloyed steel corrosion under PWR secondary side water chemistry conditions.

## 3. Methods

The material studied was low-alloyed steel with a composition (in weight percent) as follows: 0.12%C, 1.33%Mn, 0.33%Si, 0.01%P, 0.003%S, 0.15%Cr, 0.64%Ni, 0.48%Mo, 0.17%Cu, 0.02%Al, balance Fe.

Table 2 summarizes the experiments carried out in the present study. All runs were performed in PWR secondary side water ( $\text{pH}_{\text{RT}} = 9.2$ , adjusted by  $\text{NH}_3$ ) at 228°C in a recirculation water loop equipped with a 7.7 liter pressure vessel housing the test equipment and samples. All the hot parts of the loop were made of titanium. The mixed potential of the low-alloyed steel (LAS) was measured against an Ag/AgCl/0.01M KCl–reference electrode and recalculated to the Standard Hydrogen Scale (SHE). A Pt-electrode was placed close to coupons to monitor the redox-potential. In each run, a coupon specimen was exposed for weight gain/loss measurement and scanning electron microscopic (SEM) / Energy Dispersive Spectroscopic (EDS) examination. The thickness of the formed oxide was estimated from a cross-section of the coupons using scanning electron microscopy.

Electrochemical impedance spectra (EIS) of LAS were monitored in situ using the Controlled Distance Electrochemistry (CDE) arrangement (Figure 2) in the two-electrode mode with identical specimens, i.e. the upper specimen was used as both counter and reference electrode, whereas the lower specimen was used as the working electrode. In the CDE – arrangement a step motor drives a loading rod through the pressure boundary sealing. Inside the pressure vessel the movement is reduced using a soft spiral spring so that the displacement of the upper specimen can be controlled with an accuracy of about  $10^{-11}$  m/step. Normally it is enough to control the distance with an accuracy of  $10^{-7}$  m, i.e. 0.1  $\mu\text{m}$ ,

with the surface roughness of the specimen surface being about  $R_a = 1 \mu\text{m}$ . The EIS spectra were measured with a distance of  $28 \mu\text{m}$  between the electrodes.

Hydrazine was injected into the suction line of the high pressure pump of the recirculation loop, entered the 7.7 liter pressure vessel volume and was filtered out from the outflowing water by an ion exchanger. As one spectra measured with EIS takes several hours to complete, the immediate effects of hydrazine injections were followed by linear polarization resistance (LPR) measurements in a three electrode mode. One LPR measurement took about 10 minutes to complete. Also the LPR measurements were performed with a distance of  $28 \mu\text{m}$  between the electrodes.

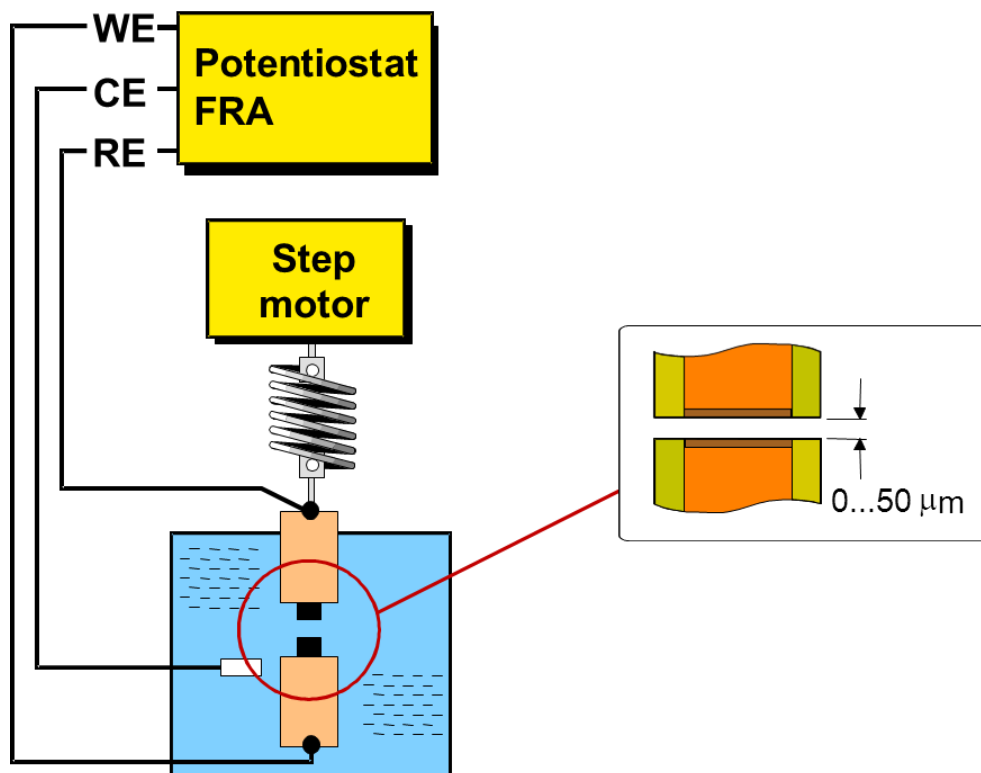


Figure 2 Schematic picture of the Controlled Distance Electrochemistry (CDE) arrangement. FRA = Frequency Response Analyser, WE = Working Electrode, CE = Counter Electrode, RE = Reference Electrode.

Table 2 Experiments performed within this study.  $T = 228^{\circ}\text{C}$ ,  $\text{pH}_{\text{RT}} = 9.2$  ( $\text{NH}_3$ ). A total of three experiments, the third one having several different stages.

<b>Experiment</b>	<b><math>[\text{N}_2\text{H}_4]</math> / ppb</b>	<b>Duration / hrs</b>
1	0	100
2	100	100
3.1	0	110
3.2	60	2
3.3	0	27
3.4	80	2
3.5	0	113
3.6	35000	2
3.7	0	52
3.8	150	20

## 4. Results

---

### 4.1 Oxide films and weight gain

The surface appearance of the sample after 100 hr exposure to water with 0.5 ppm  $\text{NH}_3$  ( $\text{pH}_{\text{RT}} = 9.2$ ) at  $T = 228^{\circ}\text{C}$  (experiment 1) is shown in Fig. 3 and the cross section in Fig. 4. A number of quite large oxide crystals (outer oxide film) are seen deposited on top of an even on-grown oxide film (inner oxide film), the thickness of which was measured to be  $0.29 \mu\text{m}$ . The coverage of the deposited layer and the average particle diameter were estimated (with Image J –software) to be  $r = 42\%$  and  $d_{\text{ave}} = 0.2 \mu\text{m}$ . The corresponding images for the experiment 2 (100 hr exposure to water with 0.5 ppm  $\text{NH}_3$  ( $\text{pH}_{\text{RT}} = 9.2$ ) + 100 ppb  $\text{N}_2\text{H}_4$  at  $T = 228^{\circ}\text{C}$ ) are shown in Figs. 5 and 6. The deposited oxide crystals were much smaller,  $d_{\text{ave}} = 0.09 \mu\text{m}$  with coverage of  $r = 32\%$ . The corresponding images for the sample that was exposed first during experiment 1 followed by exposure during experiment 2 are shown in Figs 7 and 8. The deposited oxide structure and coverage fall between the two previous ones, and the thickness of the on-grown inner oxide layer is reasonable considering the total exposure time of 200 hrs for this sample.

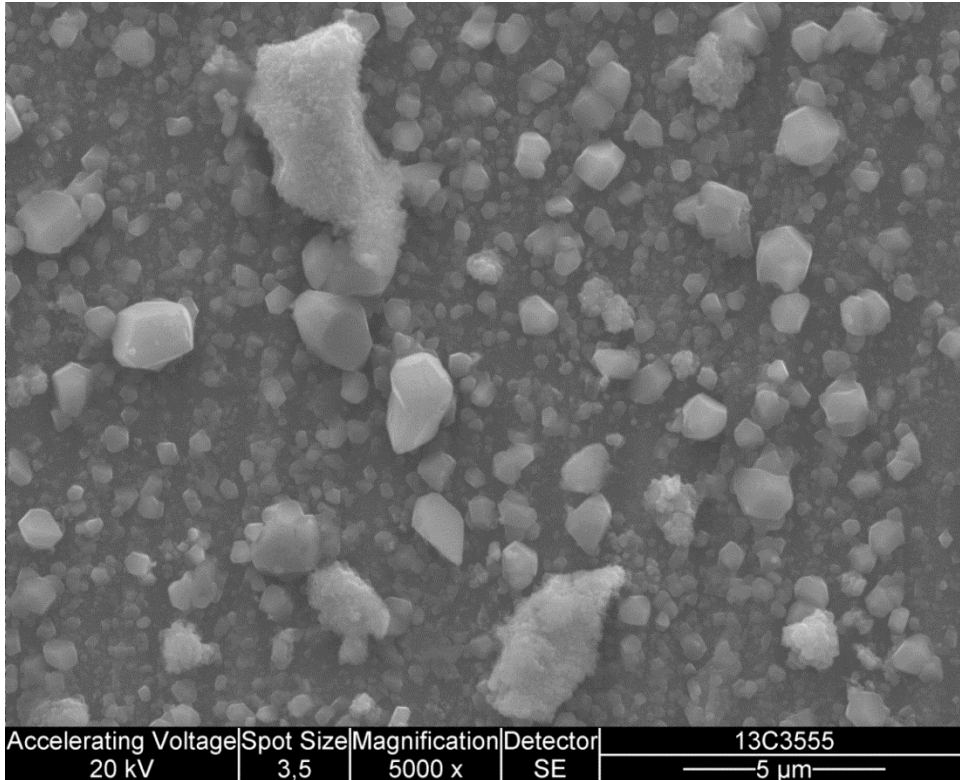


Figure 3 Surface appearance of sample after 100 hr exposure to water with 0.5 ppm  $\text{NH}_3$  ( $\text{pH}_{\text{RT}} = 9.2$ ) at  $T = 228\text{C}$ .

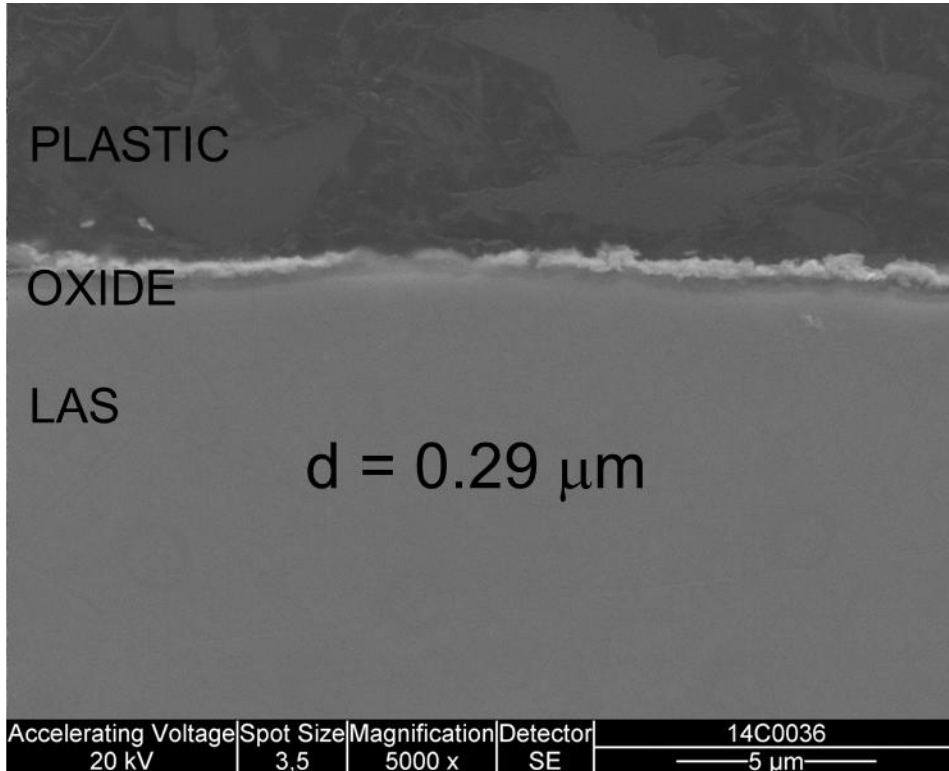


Figure 4 Cross section of the oxide film on sample after 100 hr exposure to water with 0.5 ppm  $\text{NH}_3$  ( $\text{pH}_{\text{RT}} = 9.2$ ) at  $T = 228\text{C}$ .

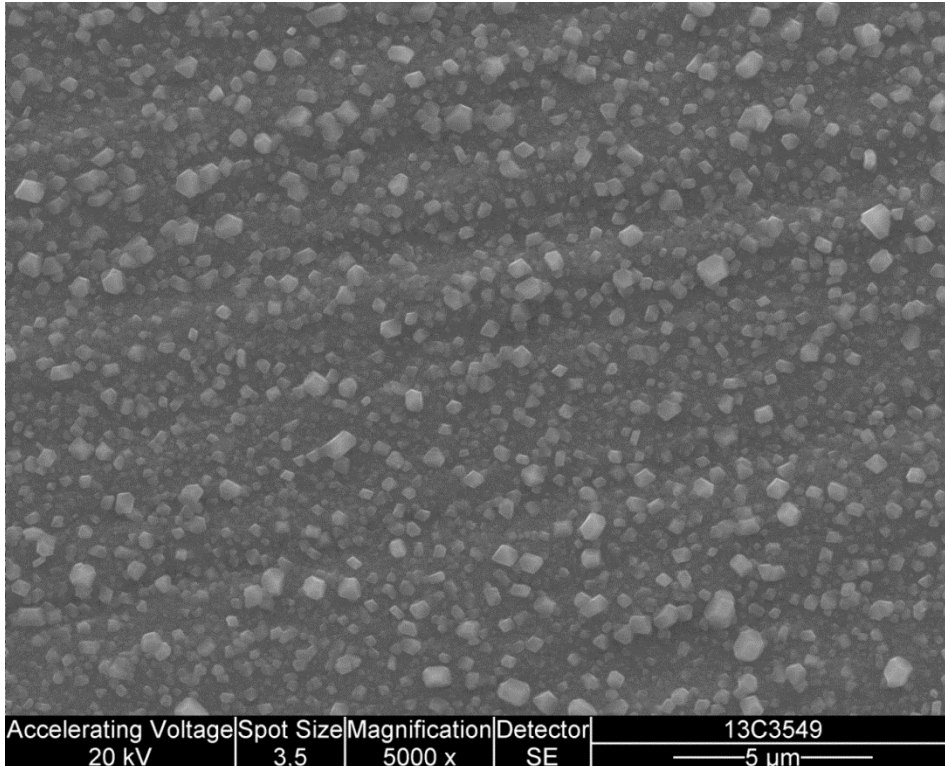


Figure 5 Surface appearance of sample after 100 hr exposure to water with 0.5 ppm  $\text{NH}_3$  ( $\text{pH}_{\text{RT}} = 9.2$ ) and 100 ppb  $\text{N}_2\text{H}_4$  at  $T = 228\text{C}$ .

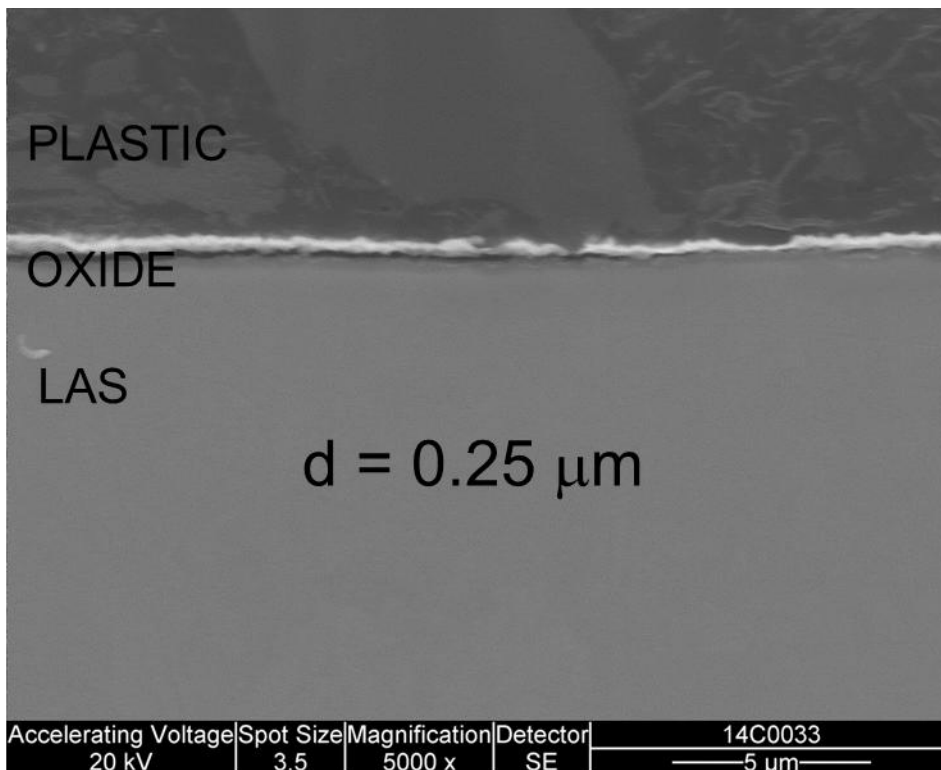


Figure 6 Cross section of the oxide film on sample after 100 hr exposure to water with 0.5 ppm  $\text{NH}_3$  ( $\text{pH}_{\text{RT}} = 9.2$ ) and 100 ppb  $\text{N}_2\text{H}_4$  at  $T = 228\text{C}$ .

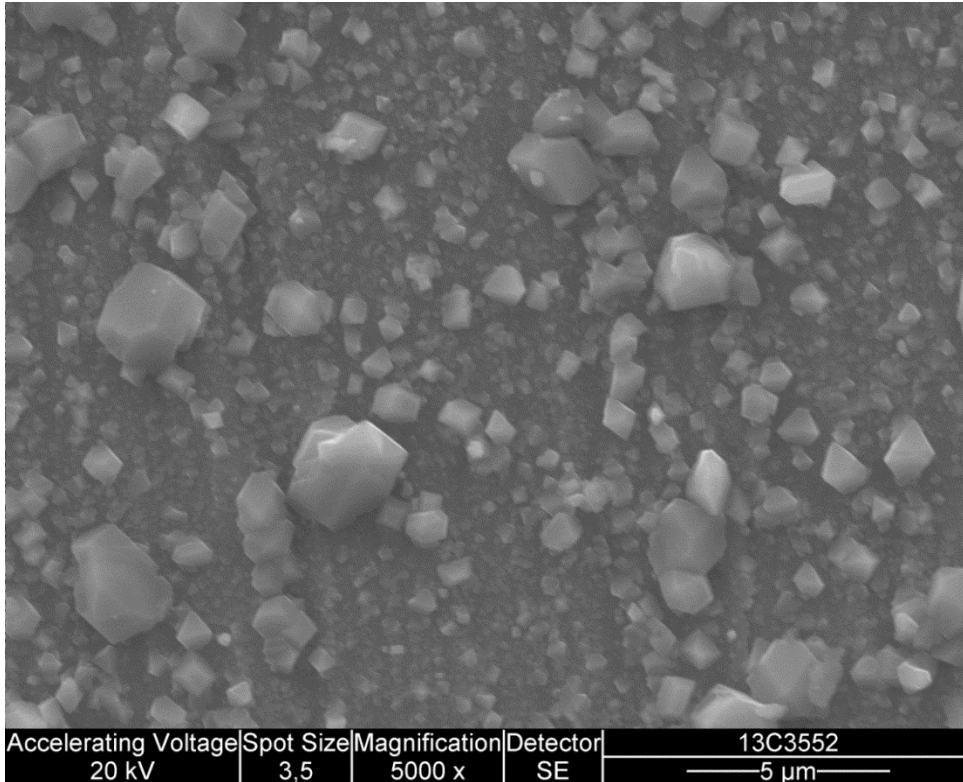


Figure 7 Surface appearance of sample after 100 hr exposure to water with 0.5 ppm  $\text{NH}_3$  ( $\text{pH}_{\text{RT}} = 9.2$ ) followed by another 100 hr exposure to water with 0.5 ppm  $\text{NH}_3$  ( $\text{pH}_{\text{RT}} = 9.2$ ) and 100 ppb  $\text{N}_2\text{H}_4$  at  $T = 228\text{C}$ .

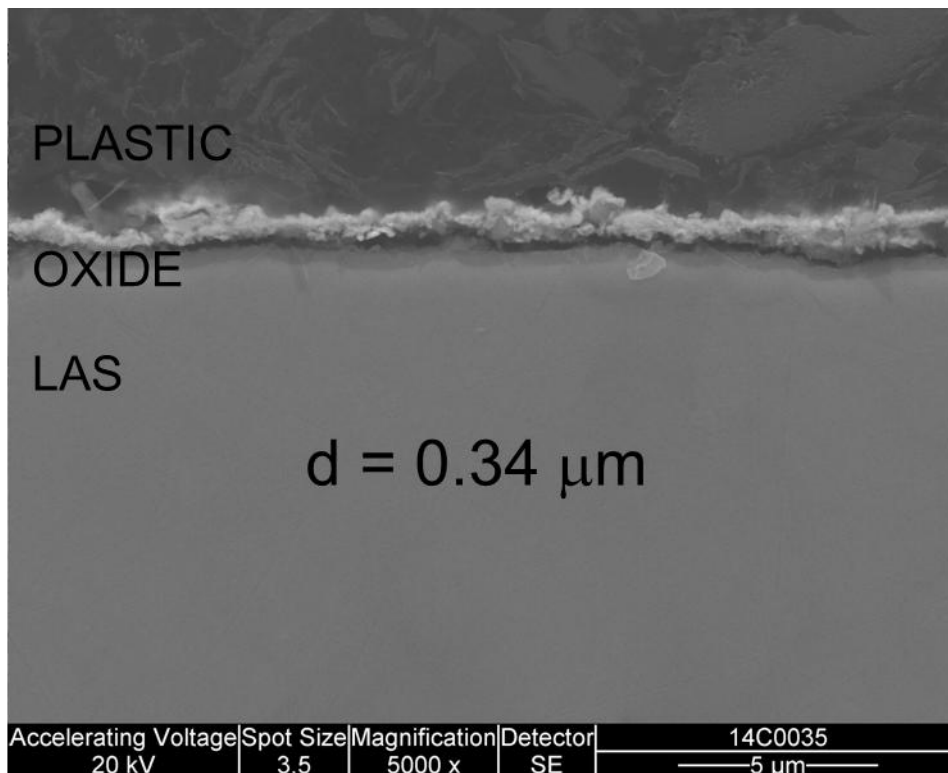


Figure 8 Cross section of the oxide film on sample after an 100 hr exposure to water with 0.5 ppm  $\text{NH}_3$  ( $\text{pH}_{\text{RT}} = 9.2$ ) followed by an 100 hr exposure to water with 0.5 ppm  $\text{NH}_3$  ( $\text{pH}_{\text{RT}} = 9.2$ ) and 100 ppb  $\text{N}_2\text{H}_4$  at  $T = 228\text{C}$ .

Corrosion rates of the samples shown in Figs 4 to 8 were calculated based on the actual measured weight loss and the estimated weight of the inner and outer oxide layers. The corrosion rates were estimated to be 15, 21 and 15  $\mu\text{m}/\text{y}$ , for the samples in experiment 1, 2 and 1+2, respectively. The corrosion rates of experiments 1 and 2 can be directly compared, as the exposure times were the same. However, the corrosion rate for the sample exposed in both experiments 1 and 2 corresponds to a total exposure time of 200 hrs, and as the corrosion rate of steels normally shows a decreasing trend as a function of time, this result is not directly comparable. Based on the weight loss the corrosion rate of LAS in presence of 0.5 ppm  $\text{NH}_3$  + 100 ppb  $\text{N}_2\text{H}_4$  was about x1.4 higher than in presence of  $\text{NH}_3$  only.

## 4.2 Impedance spectroscopy

The potentials of LAS were in all experiments well into the stability area of magnetite, i.e. below the  $\text{Fe}_2\text{O}_3/\text{Fe}_3\text{O}_4$  equilibrium potential of  $E_{\text{Fe}_2\text{O}_3/\text{Fe}_3\text{O}_4}(T=228^\circ\text{C}) = -0.42 \text{ V}_{\text{SHE}}$ . A comparison of the impedance spectra of LAS after 100 hrs exposure at  $T = 228^\circ\text{C}$  to 0.5 ppm  $\text{NH}_3$  and 0.5 ppm  $\text{NH}_3$ +100 ppb  $\text{N}_2\text{H}_4$  (experiments 1 and 2) is shown in Fig. 9. The oxide grown in the presence of hydrazine shows about 40% smaller impedance value at the low end of the frequency spectrum, which is interpreted to result in an about x1.4 higher corrosion rate for the case in which hydrazine is present. This is comparable with the corrosion rate difference calculated from the estimated weight gain 15 and 21  $\mu\text{m}/\text{y}$  for experiments 1 and 2, respectively, i.e.  $21/15 = \text{x}1.4$ .

Figure 10 shows the impedance spectra measured during experiment 3, in which an oxide film was first grown on LAS in presence of 0.5 ppm  $\text{NH}_3$  at  $T = 228^\circ\text{C}$  for about 100 hrs, and then the sample was subjected to several short term (max 2 hrs) transients with hydrazine, and finally to a longer term exposure to a hydrazine concentration of 150 ppb. It is clear from the spectra in Fig. 10 that neither the short term transients with hydrazine nor the longer term exposure to  $[\text{N}_2\text{H}_4] = 150 \text{ ppb}$  resulted in a measurable difference in the impedance magnitude. This can be interpreted so that when there is a stable oxide film on LAS grown in an environment without hydrazine, the protective properties of such a film do not change when subjected to hydrazine levels of maximum 150 ppb.

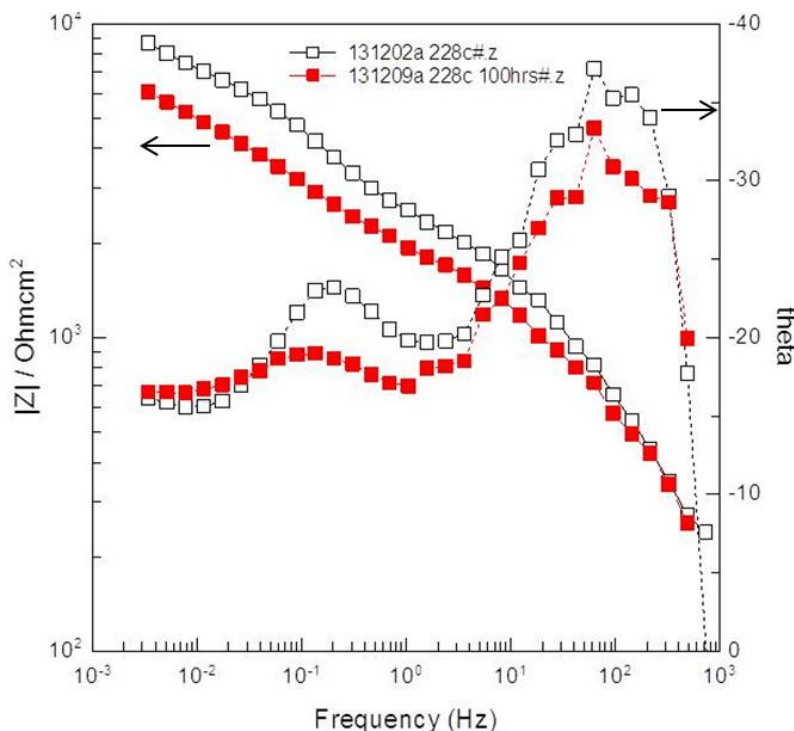


Figure 9 Comparison of the impedance spectra of LAS after 100 hrs exposure at  $T = 228^\circ\text{C}$  to 0.5 ppm  $\text{NH}_3$  (white squares) and 0.5 ppm  $\text{NH}_3$ +100 ppb  $\text{N}_2\text{H}_4$  (red squares).

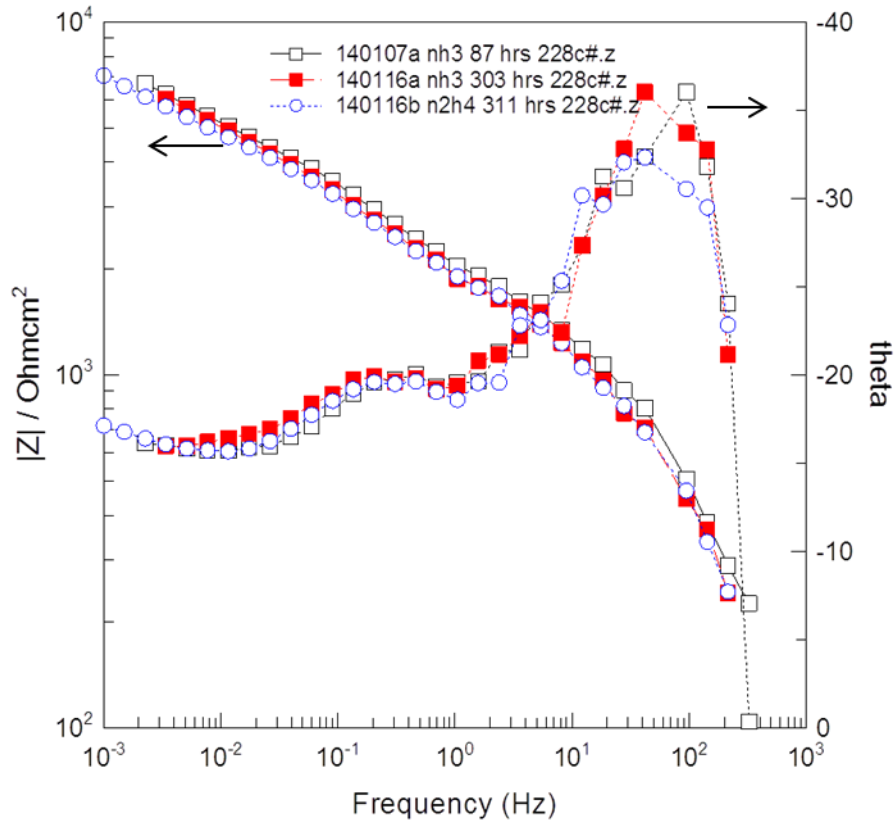


Figure 10 Comparison of the impedance spectra of LAS after 87 hrs exposure at  $T = 228^{\circ}\text{C}$  to 0.5 ppm  $\text{NH}_3$  (white squares), spectra after several hydrazine injections lasting not more than 2 hrs (red squares) and spectra about 10 hrs after permanent addition of 150 ppb  $\text{N}_2\text{H}_4$  (circles).

### 4.3 Polarisation resistance measurements during $\text{N}_2\text{H}_4$ transients

In polarisation resistance measurements the specimen is polarised  $\pm 30$  mV from the corrosion potential with a low sweep rate so that one cycle takes about 500 seconds, corresponding to a frequency of 2 mHz. The slope of the current-voltage curve, multiplied with specimen surface area is called polarisation resistance and can be used to estimate the corrosion rate of the material. The higher the polarisation resistance, the lower is the corrosion rate. In this study, polarisation resistance was used to monitor the effects of hydrazine transients on LAS corrosion, because the transients were designed to last less than two hours, thus precluding the use of impedance spectroscopy.

Figure 11 shows the result of the injection of hydrazine to about  $[\text{N}_2\text{H}_4] = 60$  ppb level. The polarisation resistance does not change markedly as a result of the injection. The same is true for the case of injection of  $[\text{N}_2\text{H}_4] = 80$  ppb and 150 ppb, shown in Figs. 12 and 13, respectively. The polarisation resistance changes are within the normal variation for repetitions with this technique. An injection to a level of about  $[\text{N}_2\text{H}_4] = 35000$  ppb shown in Fig. 14, on the other hand, resulted in a dramatic decrease of polarisation resistance (and corresponding increase in corrosion rate) by a factor of about x5. However, even in this case, when the hydrazine is removed by the ion exchanger the polarisation resistance is seen to return close to the starting level. With such a high concentration of hydrazine also the  $\text{pH}_{\text{RT}}$  and conductivity change (as estimated by MULTEQ software) from  $\text{pH}_{\text{RT}} = 9.2$  to  $\text{pH}_{\text{RT}} = 9.6$  and  $\gamma = 4.2 \mu\text{Scm}^{-1}$  to  $\gamma = 9.7 \mu\text{Scm}^{-1}$ , and thus the changes in polarisation resistance could be at least partly induced by the changes in  $\text{pH}_{\text{RT}}$  and conductivity.

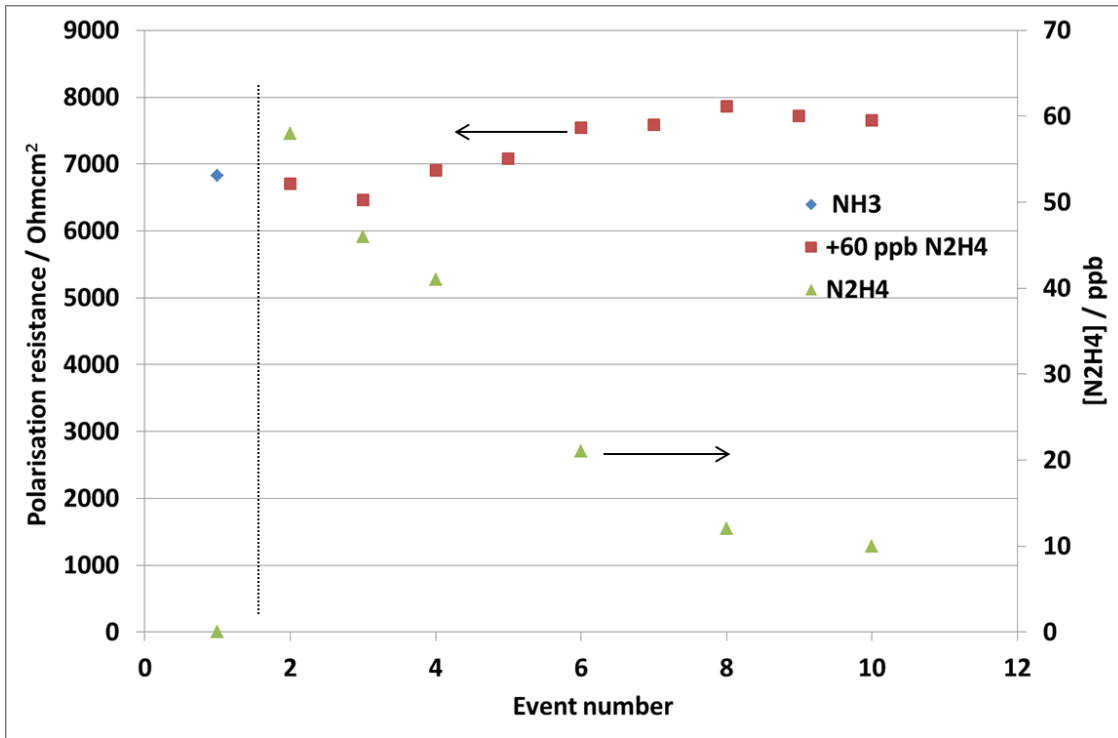


Figure 11 Polarisation resistance of LAS during a hydrazine injection to about  $[N_2H_4] = 60$  ppb.

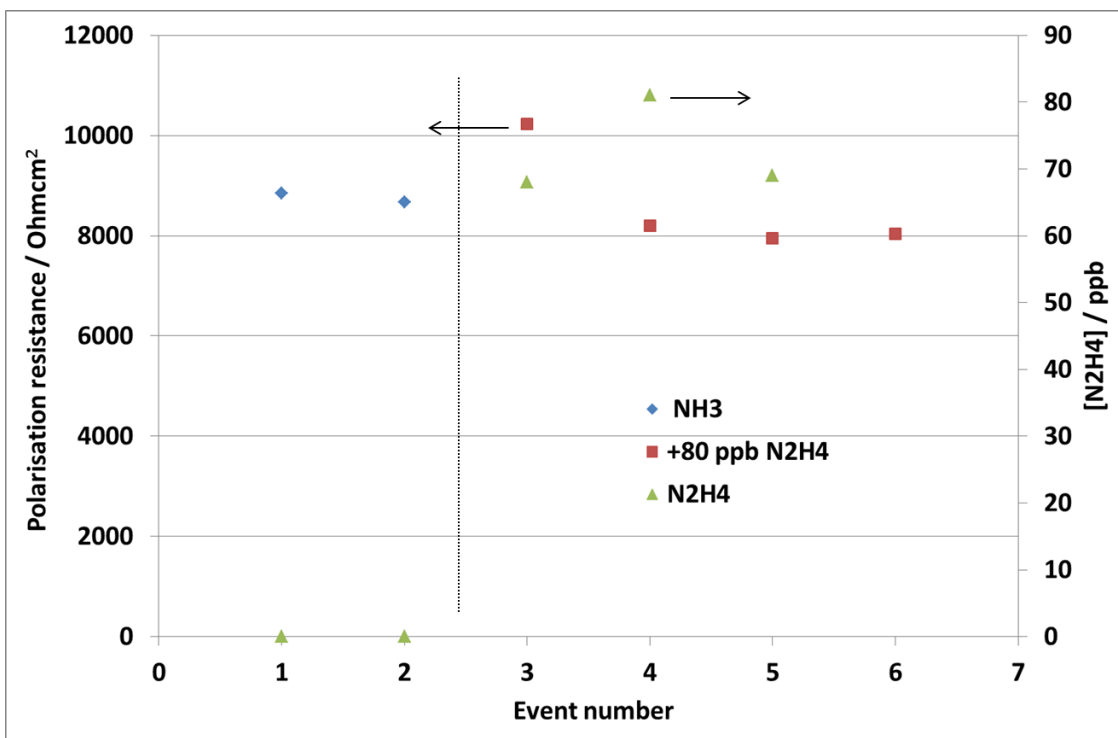


Figure 12 Polarisation resistance of LAS during a hydrazine injection to about  $[N_2H_4] = 80$  ppb.

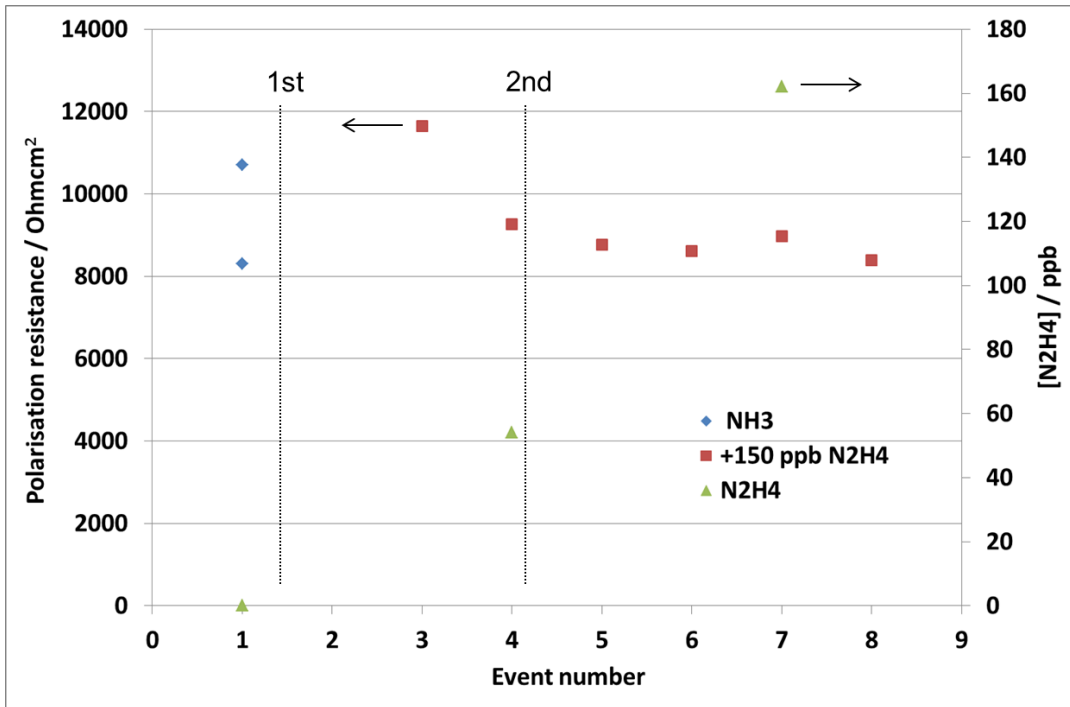


Figure 13 Polarisation resistance of LAS during a hydrazine injection first to about  $[N_2H_4] = 50$  ppb and then additionally to about  $[N_2H_4] = 150$  ppb.

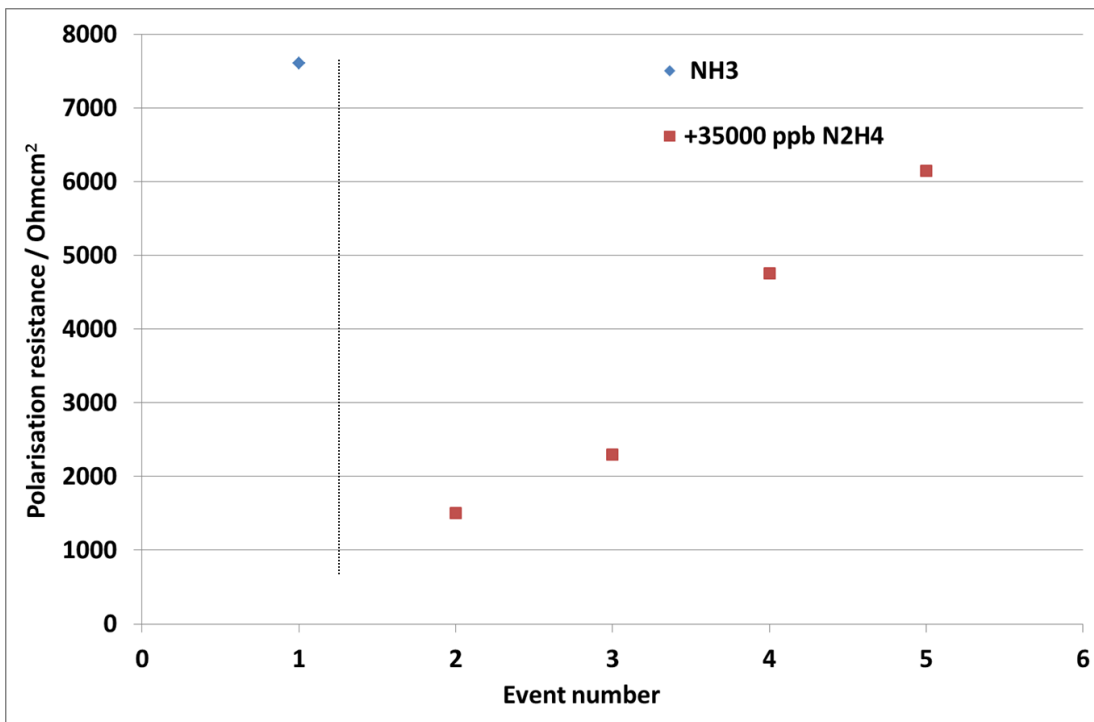


Figure 14 Polarisation resistance of LAS during a hydrazine injection to about  $[N_2H_4] = 35000$  ppb.

## 5. Validation of results

---

The number of repetitions of hydrazine injections onto LAS surface that has been previously oxidised without hydrazine is thought to be high enough for reliable conclusions. The method used to estimate the corrosion rate based on the weight loss and oxide film thickness under similar exposure times has earlier been estimated /3/ to result in an error margin of  $\pm 30\%$ . Even with such a high error margin, the estimated corrosion rates do support the result that an oxide film grown in the presence of 100 ppb hydrazine shows a less protective character and a higher corrosion rate than that grown without the presence of hydrazine. However, it is felt that more repetitions are needed to further validate the EIS (Fig. 9) and weight loss results.

## 6. Summary and Conclusions

---

The effect of hydrazine on corrosion rate of low-alloyed steel (LAS) was studied by in situ and ex situ techniques under PWR secondary side water chemistry conditions at  $T = 228^\circ\text{C}$ . Based on the results the following conclusions can be made:

- Hydrazine injection to a maximum level of 150 ppb onto previously oxidised surface does not affect the corrosion rate of LAS
- Hydrazine at the level of 100 ppb decreases markedly the amount and the size of deposited oxide crystals on LAS surface. This supports the hypothesis that hydrazine increases magnetite solubility.
- An oxide grown in the presence of 100 ppb hydrazine shows somewhat weaker protective properties resulting in a higher corrosion rate compared to an oxide film grown without hydrazine. This could explain the accelerating effect of higher concentrations of hydrazine found in flow assisted corrosion (FAC) studies of LAS. This hypothesis needs further experimental verification.

## References

---

1. Chemistry Effects on Flow-Accelerated Corrosion – Pressurized Water Reactors: Hydrazine and Oxygen Investigations. EPRI, Palo Alto, CA: 2005. 1011835.
2. Correlation of Flow Accelerated Corrosion (FAC) of Steam Generator Internals with Plant Water Chemistry, EPRI, Palo Alto, CA: 1998. TR-111113.
3. Effect of Chloride on the Oxides on Low-Alloyed Steel in Conditions of a Light Water Reactor Pressure Vessel Cladding Flaw, Martin Bojinov, Erika Nowak, Timo Saario, Konsta Sipilä and Michael Stanislowski. Journal of the Electrochemical Society, 161 (4) C177-C187 (2014).